

# Controlling atomic vapor density in paraffin-coated cells using light-induced atomic desorption

T. Karaulanov,\* M. T. Graf, D. English, S. M. Rochester, Y. J. Rosen, K. Tsigutkin, and D. Budker†  
*Department of Physics, University of California at Berkeley, Berkeley, California 94720-7300*

E. B. Alexandrov and M. V. Balabas  
*S. I. Vavilov State Optical Institute, St. Petersburg, 199034 Russia*

D. F. Jackson Kimball  
*Department of Physics, California State University – East Bay, Hayward, California 94542-3084*

F. A. Narducci  
*EO Sensors Division, US Naval Air Systems Command, Patuxent River, Maryland 20670*

S. Pustelny  
*Centrum Badań Magnetoptycznych, M. Smoluchowski Institute of Physics,  
 Jagiellonian University, Reymonta 4, 30-059 Kraków, Poland*

V. V. Yashchuk  
*Advanced Light Source Division, Lawrence Berkeley National Laboratory, Berkeley, California 94720*  
 (Dated: October 29, 2018)

Atomic-vapor density change due to light induced atomic desorption (LIAD) is studied in paraffin-coated rubidium, cesium, sodium and potassium cells. In the present experiment, low-intensity probe light is used to obtain an absorption spectrum and measure the vapor density, while light from an argon-ion laser, array of light emitting diodes, or discharge lamp is used for desorption. Potassium is found to exhibit significantly weaker LIAD from paraffin compared to Rb and Cs, and we were unable to observe LIAD with sodium. A simple LIAD model is applied to describe the observed vapor-density dynamics, and the role of the cell's stem is explored through the use of cells with lockable stems. Stabilization of Cs vapor density above its equilibrium value over 25 minutes is demonstrated. The results of this work could be used to assess the use of LIAD for vapor-density control in magnetometers, clocks, and gyroscopes utilizing coated cells.

PACS numbers: 34.50.Dy, 79.20.La

## I. INTRODUCTION

In glass vapor cells atomic polarization relaxes rapidly when atoms collide with cell walls. This relaxation can be reduced by up to four orders of magnitude by introducing a paraffin coating [1–4]. Long-lived atomic polarization (relaxation times of seconds have been observed) enables extremely sensitive measurements of magnetic fields [3–7], enhances nonlinear optical effects at low light powers (see the review [8] and references therein), and may make possible precision tests of fundamental symmetries [9–11]. In addition to these applications, paraffin-coated cells have been used in the study of light propagation dynamics [12, 13], for generation of spin-squeezed states [14], quantum memory for light [15], quantum teleportation [16], and creation and study of high-rank polarization moments [17, 18]. There has also been renewed interest in the application of paraffin-coated cells in minia-

turized atomic clocks, magnetometers, and gyroscopes [19, 20]. In spite of their wide and varied application and several detailed studies of their spin-relaxation properties [2, 21–26], there is still much to learn about the paraffin-coated cells.

In this work, we investigate a possibility to affect density changes in coated cells using light-induced atomic desorption (LIAD) [27, 28]. The effect was first investigated in paraffin-coated cells in Refs. [29, 30]. Compared to the earlier work, we extend the spectral range of the desorbing light into the ultraviolet, and look at LIAD with potassium (K), comparing the effect to that with Rb and Cs. We also test for LIAD in sodium (Na). Using cells with lockable stems (uncoated side-arms containing metallic alkali samples), we elucidate the role of the stem in the LIAD dynamics.

LIAD is a process in which alkali atoms are desorbed from the walls of a (in our case, coated) vapor cell into the volume of the cell when the cell is exposed to light of sufficiently short wavelength and sufficient intensity. This is possible because, over time, alkali atoms are adsorbed into the coating, and can be released by the action of the desorbing light. The LIAD phenomenon has been

\*Electronic address: karaulanov@berkeley.edu

†Electronic address: budker@berkeley.edu

observed using a wide range of surfaces, besides paraffin: sapphire [31–33], silane-coated glass (in particular, polydimethylsiloxane (PDMS) ) [27, 28, 34–37], superfluid  $^4\text{He}$  films [38, 39], quartz [40], porous silica [41], and octadecyltrichlorosilane (OTS) [42, 43]. Rubidium LIAD from a octadecyldimethylmethoxysilane (ODMS) coating within a photonic band-gap fiber was also demonstrated [44] allowing for realization of efficient nonlinear interactions (in this case, electromagnetically induced transparency) at ultra-low optical power. Paraffin coatings are particularly useful because of the aforementioned long spin relaxation times, while LIAD is an attractive method for rapid control of atomic density.

The change in vapor density produced by LIAD in a paraffin coated cell depends on many factors including the cell’s geometry, the wavelength of the desorbing light, the alkali vapor used and the cell’s history, see, for example, Ref. [29]. Important geometrical factors are the volume, surface area, and stem-opening area. The latter is of importance because of the so-called “reservoir” effect [2]. The stem of the cell acts either as a source or a sink for atoms in the volume of the cell depending on whether the vapor density in the volume is lower or higher than that in the stem. Thus the ratio of dimensions, particularly that of the area of the stem opening to the surface area of the cell, dictates, to a large degree, the time scale for which the excess density created by LIAD will persist before atoms retreat to the stem. The reservoir effect is most pronounced in small cells since they have the smallest internal surface area but often have stem openings that are comparable to those of larger cells, so that the stem-opening to surface-area ratio is particularly unfavorable.

Some applications such as compact, sensitive atomic magnetometers, clocks, and gyroscopes require high vapor densities. This is because small cells require higher densities to achieve reasonably sized signals. In these cases, heating is of limited use with paraffin coated cells since the temperature cannot exceed 60 – 80°C without melting the coating. Is LIAD, then, a possible solution for achieving high density? If so, what is to be done about the reservoir effect? As a result of the present investigation, the answer is affirmative, particularly with UV light for high-efficiency LIAD, and using lockable-stem cells to mitigate the reservoir effect.

The structure of the paper is as follows: parameters describing the LIAD dynamics along with a simple model of LIAD processes are summarized in Sec. II; the experimental apparatus are described in Sec. III; the effect is studied for the visible desorbing light in Rb and Cs in Sec. IV and in K and Na in Sec. V; the case when UV irradiation is used in K and Rb cells is explored in Sec. VI; tests with different paraffin coatings are presented in Sec. VII. In Sec. VIII demonstration of the control over the Cs density using LIAD is performed. Finally, discussion and conclusion are presented in Sec. IX.

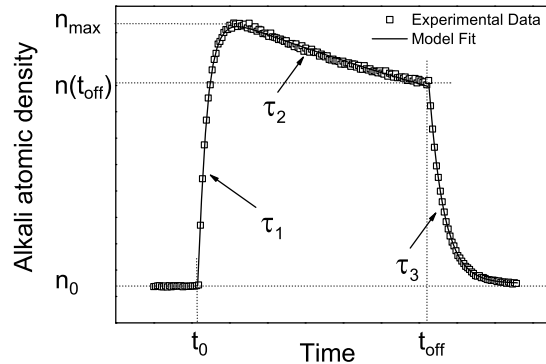


FIG. 1: Typical LIAD signal and a model fit. The times when the desorption light is turned on and off are denoted as  $t_0$  and  $t_{\text{off}}$ . The initial  $n_0$ , maximum  $n_{\text{max}}$  and  $n(t_{\text{off}})$  densities are indicated. The three characteristic timescale constants are  $\tau_1$ ,  $\tau_2$  and  $\tau_3$ .

## II. LIAD DYNAMICS AND ITS CHARACTERIZATION

Typical LIAD temporal behavior is illustrated in Fig. 1. We see three distinct regions: a rapid rise of alkali-vapor density in the volume of the cell after the desorbing light is turned on at time  $t_0$ , a slow subsequent fall-off and a rapid decay of the vapor density once the light is turned off at time  $t_{\text{off}}$ .

In Ref. [29], a model describing most salient features in the LIAD dynamics was introduced. It is based on the rate equations and establishment of equilibrium for the atomic vapor density between the cell volume and the stem before, during and after the desorbing light action on the paraffin coated alkali cell. A number of phenomenological parameters are introduced in the model: vapor density in the stem of the cell, flux of atoms adsorbed into the coating, exchange rate between the stem and the volume of the cell, the number of free atoms in the coating, the rate of irreversible loss of atoms to the glass or impurities, light-independent flux of atoms from the surface into the cell volume, induced desorption rate, etc.

While this model is successful in describing LIAD dynamics in detail, its significant drawback is the large number of parameters. Since the focus of the present research is practical applications of LIAD, we have adopted a greatly simplified version of the model in which only the most prominent features of LIAD dynamics are described but the number of fitting parameters is minimized. The effects that are not accounted for include, for example, “undershooting” of the vapor density below its original level after the desorbing light is turned off. These effects are not prominent under the experimental conditions employed here.

We define a set of phenomenological parameters that describe the LIAD dynamics. The maximum change of the atomic density in the volume of the vapor cell is  $\Delta n = n_{\max} - n_0$ , where  $n_{\max}$  is the maximum value of the density reached after the cell is illuminated by desorbing light, and  $n_0$  is the initial density prior to illumination. The maximum LIAD yield is defined as relative change of the density  $\eta = \Delta n/n_0$ . There are three different time scales for the LIAD dynamics. The first, shorter time scale with a time constant  $\tau_1$  characterizes the exponential growth of the alkali-vapor density in the cell volume just after the desorbing light is switched on. The second, longer time scale with time constant  $\tau_2$  characterizes the decrease in density while the desorbing light is still on. A third time constant  $\tau_3$  is introduced to account for density relaxation back to its equilibrium value in the absence of the desorbing light. Note that in Ref. [29] it was found that the density drops slightly below the initial value  $n_0$  after the light is turned off and eventually recovers on a much longer time scale. We ignore this effect here. In Ref. [29] using a more detailed model, it is shown that the times  $\tau_1$  and  $\tau_2$  both depend on the desorbing light intensity. The loss of atoms from the volume of the cell to the stem also plays an important role in establishing the time scales  $\tau_1$  and  $\tau_2$  [29]. In the present work, using lockable-stem cells, we directly verify this.

We use a simple model to describe the LIAD dynamics, in which the time evolution of the atomic density in the volume of the cell  $n(t)$  is described by the following equation:

$$n(t) = \begin{cases} n_0 + N \left(1 - e^{-\frac{(t-t_0)}{\tau_1}}\right) e^{-\frac{(t-t_0)}{\tau_2}} & , t_0 \leq t \leq t_{\text{off}} \\ n_0 + (n(t_{\text{off}}) - n_0) e^{-\frac{(t-t_{\text{off}})}{\tau_3}} & , t > t_{\text{off}}. \end{cases}$$

where the relation between  $N$  and  $\Delta n$  is given by

$$N = \Delta n \left(1 + \frac{\tau_1}{\tau_2}\right) \left(1 + \frac{\tau_2}{\tau_1}\right)^{\frac{\tau_1}{\tau_2}}.$$

The moments  $t_0$  and  $t_{\text{off}}$  correspond to the times when the desorption light is switched on and off. The time evolution corresponding to the equation above is fit to the experimental data, in this way determining  $\tau_1$ ,  $\tau_2$  and  $\tau_3$ .

### III. APPARATUS AND EXPERIMENTAL SETUP

The parameters of the paraffin-coated alkali-vapor cells used in this work (including the ones shown in Fig. 2) are summarized in Table. I. The stem openings are circular with a diameter of  $\sim 1$  mm. The cells contain a drop of an alkali metal in their stems. In the case of lockable-stem cells, a freely moving glass bullet inside the stem is used to open and close the stem opening by rotating

TABLE I: Cells used for the LIAD study. For a given alkali atom the cell stem type, shape, diameter (D), and length (L) are specified.

Atom, stem type	Shape	D [mm]	L [mm]
Cs, lockable	cylindrical	20	30
$^{85}\text{Rb}$ , lockable	cylindrical	20	20
K, lockable	spherical	50	–
Na, non-lockable	cylindrical	50	70

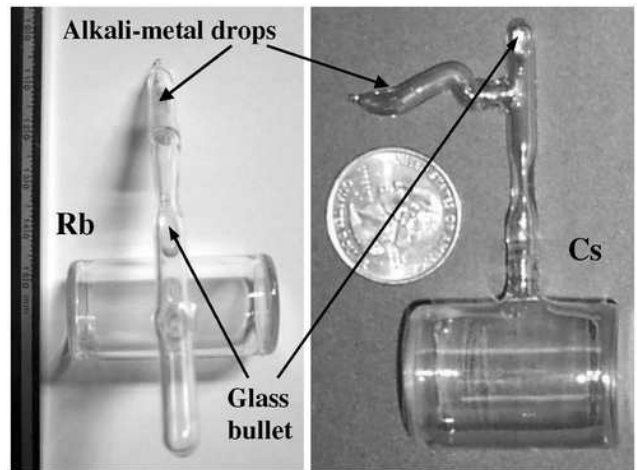


FIG. 2: Photographs of the Rb and Cs cells with lockable stems.

the cell 180° about its axis and allowing the bullet to slide due to gravity. Special mounts were designed to allow for consistent locking and unlocking of the stems. A description of the procedure of coating and filling the cells can be found in Ref. [29]. Figure 3 illustrates the general setup of the experiment. For all the cells there is a probe beam which is resonant with the transition of the particular alkali atom. For the Cs cell, the beam which is resonant with the Cs D2 transition originates from a 852-nm extended-cavity diode laser. For the Rb cell, the beam resonant with the Rb D1 transition is derived from a 795-nm EOSI 2010 extended-cavity diode laser system. The probe laser for the K D1 line is a 770 nm - New Focus Velocity diode-laser systems. Typical light power of the probe beams is  $5 \mu\text{W}$  and the diameter is  $\approx 3$  mm. In the case when Na is studied a collimated beam originated from a Na hollow cathode lamp is used. The probe beam passes through the cell and falls on a photodiode outfitted with an band-pass interference filter with a 12-nm FWHM centered near the transition wavelengths which prevents detection of scattered light from the light sources used for desorption. Scanning the probe laser (in all the cases except for Na), we record absorption profiles that are subsequently analyzed to extract the alkali-vapor density in the cells. The  $\text{Ar}^+$  laser (operating at the 514 nm line), is employed for desorption in the visible range (see Fig. 3a). The desorb-

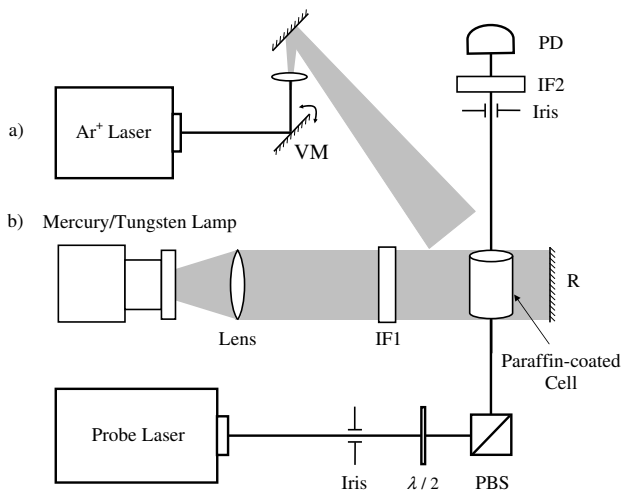


FIG. 3: Diagram of the experimental setup used in LIAD measurements. Desorption light in the visible spectrum is generated by an  $\text{Ar}^+$  laser at 514 nm - case a), while in the UV range mercury or tungsten discharge lamps are used - case b), respectively. Half-wave plate ( $\lambda/2$ ) and polarizing beam splitter (PBS) form a variable attenuator for the probe light. Interference filters IF1 are used to select the desired desorption wavelength, while IF2 filters are centered at the alkali atomic resonance lines and are used to reject the scattered light from the desorption sources. A vibrating mirror (VM) is used to average the speckle from the  $\text{Ar}^+$  laser. A reflector (R) increases the average desorption intensity falling on the surface of the paraffin cell.

ing laser beam is reflected from a vibrating mirror which serves to average the interference pattern in the laser light (speckle), and expanded using lenses in order to illuminate the entire cell. The total intensity of the desorption light (including the retroreflection) incident on the cell ranged from  $1.1 \text{ mW/cm}^2$  to  $110 \text{ mW/cm}^2$ . The LIAD experiments in the UV range were performed using 365-nm light produced by a mercury lamp (Blak-Ray B100 AP) shown on Fig. 3b. A McPherson 661A-3 high-pressure tungsten-lamp system (Fig. 3b) was used for UV excitation at 313 nm. Interference filters centered at 365-nm (FWHM=60 nm) and 313-nm (FWHM=25 nm) were used to select the desired wavelength.

#### IV. LIAD IN Rb AND Cs CELLS WITH LOCKABLE STEMS AND VISIBLE LIGHT

In order to circumvent the reservoir effect, cells with lockable stems were used. The stems in these cells can be opened or closed externally, without opening the cell. In the open-stem configuration, the cell approximates a typical paraffin-coated cell with a stem, while in the closed configuration it approximates a cell with no stem. We have experimented with Rb and Cs.

For these cells, we sought first to gather evidence of the

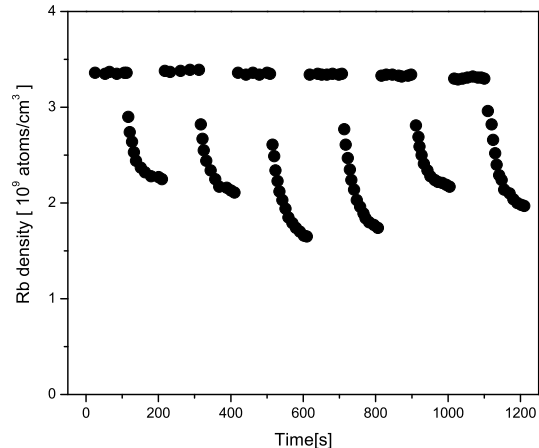


FIG. 4: Change of the Rb vapor density in the volume of the lockable-stem cell with the stem alternately open and closed. Higher densities correspond to the open configuration. The difference in the closed-stem equilibrium densities is probably due to a variation of how tightly the stem is closed with different orientation of the glass bullet.

reservoir-effect dependence on the area of the stem opening. To do this, we alternately opened and closed the stem of the Rb cell (without using LIAD) and recorded the corresponding vapor densities (Fig. 4). It is immediately apparent from the graph that there is a time dependent density drop once the stem is closed which we attribute to adsorption of alkali atoms into the coating. After a number of repetitions, the density with the stem open remains constant at about  $3.4 \times 10^9 \text{ atoms/cm}^3$ . The density with the stem closed, however, appears to have different modes (one at  $\sim 2.2 \cdot 10^9 \text{ atoms/cm}^3$ , another at  $\sim 1.8 \times 10^9 \text{ atoms/cm}^3$  and the third at  $\sim 2 \times 10^9 \text{ atoms/cm}^3$ ). These modes are most likely the result of different (but relatively stable) configurations of the glass bullet blocking the part of the stem containing the Rb metal. Similar behavior is observed with the other lockable-stem cells used. Next, we tested LIAD in Cs and Rb in both open and closed stem configurations at desorbing laser intensity of  $28 \text{ mW/cm}^2$  for Cs and  $50 \text{ mW/cm}^2$  for Rb. The LIAD dynamics in the case of Cs is presented in Fig. 5 and in the case of Rb in Fig. 6. Model fits are also presented on the figures and estimated parameters are summarized in Table. II. As already commented in Ref. [29], the stem of the cell plays a crucial role in the LIAD dynamics and characterization. In both cells, the closed-stem configuration shows considerably higher yield of LIAD for controlling the vapor density in comparison with the open configuration. The ratio of the yield  $\eta$  for these two configurations is 9 for the Cs cell and 31 for the Rb cell. Moreover, an important feature is that the rate of relaxation of the atomic density to its initial value (that before the desorbing light is turned on)

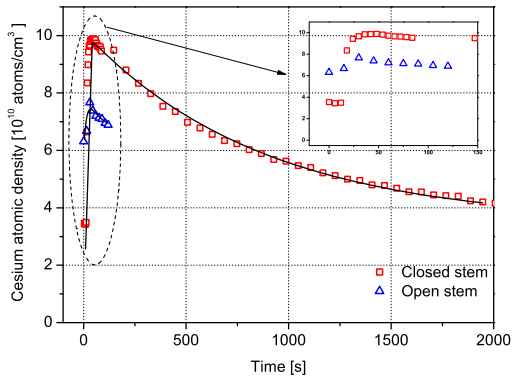


FIG. 5: (Color online) Change of the atomic density with LIAD effect in two configuration: open and closed stem in a Cs paraffin-coated locking-stem cell. The solid line represent a fit to the data. The applied desorbing light intensity was  $28 \text{ mW/cm}^2$  in both cases. The desorbing light was turned on (around  $t=15 \text{ s}$ ) and is never turned off for these measurements.

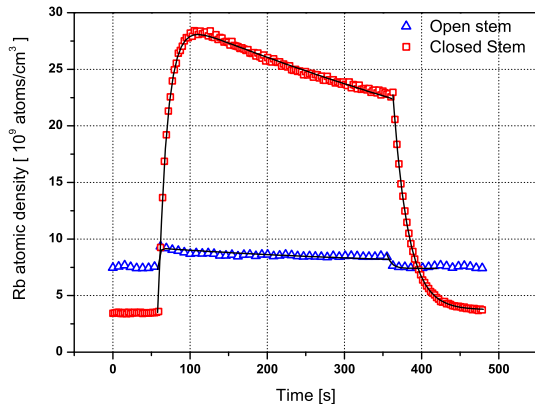


FIG. 6: (Color online) Density change with LIAD in the Rb paraffin-coated lockable-stem cell. Two cases are shown: open stem and closed stem configurations. The solid lines represent the fits to the data. The applied desorbing light is with intensity of  $50 \text{ mW/cm}^2$  in both cases. The desorbing light was turned on (around  $60 \text{ s}$ ) and then turned off (around  $360 \text{ s}$ ).

is greatly reduced when the stem is closed. Both alkalis show  $\tau_2$  values of the order of 1000 seconds with closed stems, while this time is reduced approximately by an order of magnitude with open stems.

TABLE II: LIAD characterization parameters extracted from the model fit to the LIAD experimental data. The maximum LIAD yield  $\eta$ , the  $\tau_1$ ,  $\tau_2$  and  $\tau_3$  relaxation times of the atomic density are presented for the Rb and Cs cells in open (Rb - o, Cs - o) and closed (Rb - c, Cs - c) stem configurations. The desorption light used is characterized by wavelength ( $\lambda$ ) and intensity ( $I$ ).

Cell	$\lambda$ (nm)	$I$ (mW/cm <sup>2</sup> )	$\eta$	$\tau_1$ (s)	$\tau_2$ (s)	$\tau_3$ (s)
Cs - o	514	28	0.22	18(3)	62(6)	–
Cs - c	514	28	1.9	7.1(4)	869(22)	–
Rb - o	514	50	0.25	2.0(3)	370(9)	6(1)
Rb - c	514	50	7.7	11.8(1)	918(9)	19.7(1)
Rb - o	365	5	0.42	1.9(3)	331(6)	1.6(1)
Rb - c	365	5	7.5	13.3(2)	1185(29)	17.4(3)
Rb - c	313	0.25	2.4	27.9(2)	1302(14)	32.5(2)

## V. LIAD IN K AND Na CELLS WITH VISIBLE LIGHT

An attempt was made to detect LIAD in K. With  $30 \text{ mW/cm}^2$  of 514-nm desorption light we were not able to register a change in potassium density. The upper limit for the weak LIAD effect that may exist in this case is  $\Delta n \sim 5 \times 10^7 \text{ atoms/cm}^3$ . Desorbing light of  $200 \text{ mW/cm}^2$  caused an increase of the density of K by  $\sim 0.2 \times 10^9 \text{ atoms/cm}^3$ . A certain amount of this change of the density may be attributable to heating of the cell. The LIAD experiment in a Na cell with a normal stem did not show any observable change of the atomic density. Both alkalis have low saturated vapor pressure at room temperature in comparison with Rb and Cs. This may affect the process of “ripening” of the coating [29, 45]. Perhaps in these cases, the number of free atoms in the coating ready to be desorbed is small and eventually they are trapped in sites with deeper interaction potentials. If this is the case, it explains why we do not observe LIAD from Na and K in the visible region – Note, however, that we do observe K LIAD with UV light (Sec. VI). Recently, we became aware of a study [46] of LIAD in a Na paraffin coated cell. In this work, a small change of the sodium density of  $2.9 \times 10^8 \text{ atoms/cm}^3$  was observed with  $3.5 \text{ W/cm}^2$  of desorbing-light intensity at 514 nm. Note that this intensity is higher by a factor of a hundred than the maximum intensity used (where the data is reliable) in our work. These results are consistent with our observations.

## VI. K AND Rb LIAD IN THE ULTRAVIOLET RANGE

Earlier work on LIAD from paraffin [29] showed that the efficiency of LIAD increases towards shorter wavelengths of desorbing light. This important fact may be

a clue to better understanding the processes involved in LIAD. To our knowledge, LIAD has not been studied in detail for excitation with light of wavelength shorter than 400 nm. In Ref. [47], the desorption dynamics in a PDMS coated Rb cell was explored under the action of a broad-spectrum light from a mercury-discharge lamp. However, wavelength selectivity in the UV spectral range was not specified. Recently, UV light at 395 nm and 253 nm was used for LIAD-assisted loading of magneto-optical traps [48] for Rb and K atoms. The authors of this work used uncoated surfaces - quartz cell walls and the walls of a stainless-steel chamber. Here we investigate LIAD in paraffin-coated rubidium and potassium cells with desorbing light at 365 nm and 313 nm. We separately discuss the study of K and Rb because no strong evidence for existence of LIAD was found for K with 514-nm excitation with desorbing-light intensity up to 200 mW/cm<sup>2</sup>. The short-wavelength limit (313 nm) for the desorption light is due to the absorption of molyglass, the material of the cells.

### A. Case of Rb

The Mercury lamp was first used as the desorption-light source with the filter centered at 365 nm. We were able to apply up to 5 mW/cm<sup>2</sup> to the Rb cell. The results with the closed and open stem are presented in Fig. 7a. The parameters from the model fit are presented in Table. II. The maximum observed change in the density in the closed-stem case is from  $4 \times 10^9$  to  $34 \times 10^9$  atoms/cm<sup>3</sup>. For comparison, to obtain a similar more than eight-fold increase of atomic density ( $\eta = 7.5$ ) using light at 514 nm with the same cell, an order of magnitude higher intensity of  $\simeq 55$  mW/cm<sup>2</sup> is needed. Both  $\tau_1$  and  $\tau_2$  times are comparable to the case of desorption by visible light at 514 nm and intensity of 50 mW/cm<sup>2</sup>. In the open-stem case, the maximum density reached is less than twice the initial density ( $\eta = 0.42$ ). In Fig. 7b, the excitation with 313-nm light (FWHM=25 nm) with intensity of only 0.25 mW/cm<sup>2</sup> is presented. In the case when the stem is open, the LIAD effect is undetectable. However, when the stem is closed, strong increase of atomic density ( $\eta = 2.4$ ) is achieved. The dynamics in both cases of UV excitation is adequately described with the model used for the visible range.

### B. Case of K

The Mercury lamp was used as the source of desorbing light with the filter centered at 365 nm and intensity at the cell of  $\sim 8$  mW/cm<sup>2</sup>. The experimental results are presented in Fig. 8. In contrast with the case when 514-nm desorbing light was used, there is an observable LIAD with UV light. This once again illustrates the fact that the efficiency of LIAD increases towards UV. In the case of K, in contrast to all other data, our model does

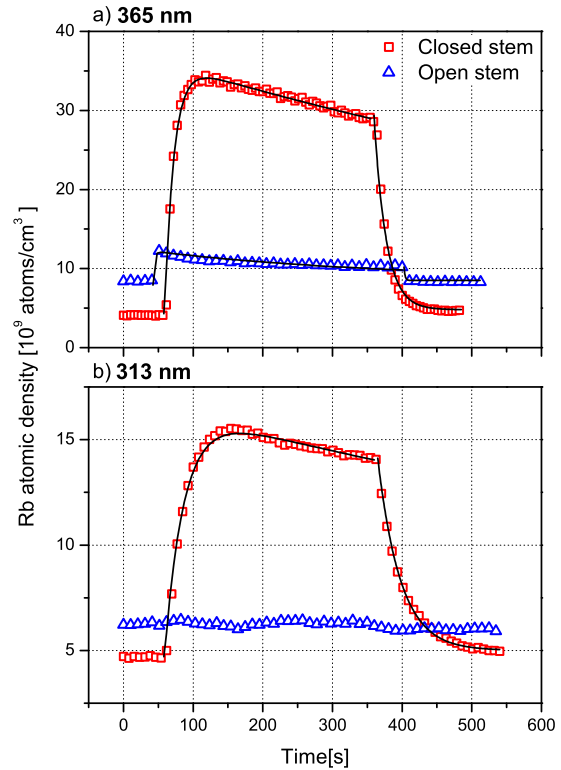


FIG. 7: (Color online) Atomic-density dynamics in a paraffin coated <sup>85</sup>Rb cell with lockable stem in case of a) 365 nm desorbing light with intensity of 5 mW/cm<sup>2</sup> and b) 313 nm at 0.25 mW/cm<sup>2</sup>. The abrupt kinks in the plots correspond to the opening and closing of the desorbing light. Note the differences in the initial densities.

not describe the entire temporal profile of the vapor density. However, fitting the fast rising and falling slopes only (closed stem configuration), we extract the maximum yield  $\eta=2.3$ ,  $\tau_1=1.7(4)$  s and  $\tau_2=4$  s. Note a drastic difference in the LIAD dynamics from what is observed with Rb: the times  $\tau_1$  and  $\tau_2$  are both much shorter, and there is no significant difference between the open- and closed-stem cases.

## VII. LIAD PERFORMANCE OF DIFFERENT TYPES OF PARAFFIN COATINGS

We tested non-lockable-stem cells containing two different types of paraffin wax. This experiment was performed to determine to which extent LIAD parameters depend on the specific type of paraffin used for coating. There are four 3.5-cm diameter spherical cells in this experiment which we will label cells 1–4, respectively. All these cells were made using the method described in Ref. [29] and contain Rb with natural isotopic abundance. Cells 1 and 2 were coated with the same paraffin as used

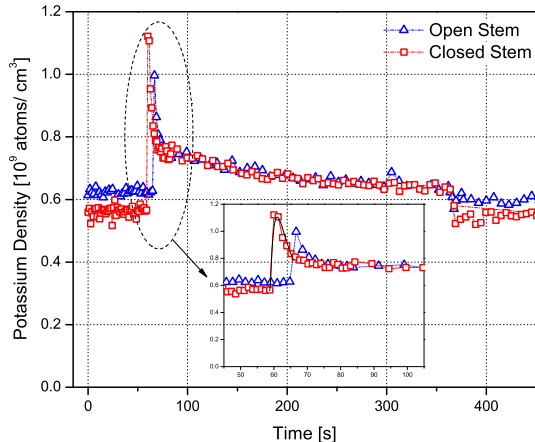


FIG. 8: (Color online) Atomic density dynamics in the paraffin-coated K cell with lockable stem in case of 365-nm desorbing light with intensity of 8 mW/cm<sup>2</sup>. The horizontal offset of the peaks is due to the difference in the time when the desorbing light was applied.

TABLE III: LIAD in Rb cells with different paraffin coatings. The cell number; paraffin type; the initial density of atoms  $n_0$ ; the maximum change of the atomic density  $\delta n$ ; and the maximum LIAD yield  $\eta$  are listed. Desorbing light at 514 nm with intensity of 74 mW/cm<sup>2</sup> was used.

Cell number	Paraffin type	$n_0$ (10 <sup>9</sup> cm <sup>-3</sup> )	$\delta n$ (10 <sup>9</sup> cm <sup>-3</sup> )	$\eta$
1	Ref.[29]	2.3	1.2	0.5
2	Ref.[29]	2	1	0.5
3	Luxco wax F/R130	1.8	1	0.6
4	Luxco wax F/R130	1.8	0.5	0.3

in the lockable-stem cells and the cells used in Ref. [29]. Cells 3 and 4 were coated with a different paraffin (Luxco wax F/R130). The cells were exposed to 514-nm light with an intensity of 74 mW/cm<sup>2</sup>. On the first trial only Cell 1 showed any response to the desorbing light. After baking the cells overnight at 70° C all the cells showed significant improvement of their LIAD properties. The results are summarized in Table. III. The results indicate that both paraffins are similar in their LIAD properties. However, the process of “ripening” plays an essential role in the desorption properties of the coating. This leads to a conclusion that cell preparation and history can significantly change the observed LIAD properties.

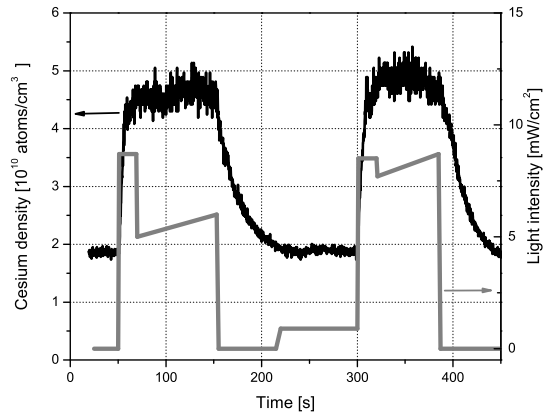


FIG. 9: Demonstration of switching of Cs atomic density using LIAD with a lockable-stem cell (stem closed). The intensity of the desorbing 405-nm light (FWHM=15 nm) is shown on the lower trace.

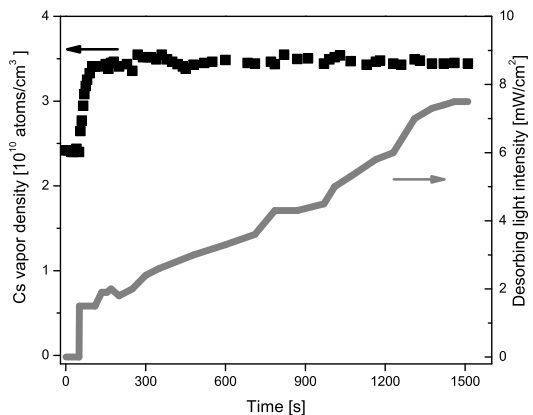


FIG. 10: Demonstration of Cs atomic density stabilization using LIAD with lockable-stem cell (stem closed). The intensity of the desorbing 405-nm light (FWHM=15 nm) is shown on the lower trace.

## VIII. CONTROL OF ATOMIC DENSITY USING LIAD

In order to demonstrate the use of LIAD for controlling atomic density, we performed two experiments with the lockable-stem Cs cell. The source of the desorbing light in both cases was an array of four light-emitting diodes (LEDs) with central wavelength of 405 nm (FWHM = 15 nm). The LED-array light intensity is modulated via changing the current. In Fig. 9 a two-pulse desorption sequence is demonstrated. In this case, the initial light intensity for both pulses is the maximum available  $\approx 9$  mW/cm<sup>2</sup> used to minimize the density ramp-up time  $\tau_1$ . In this way, relatively fast switching time of  $\approx 2$  s for

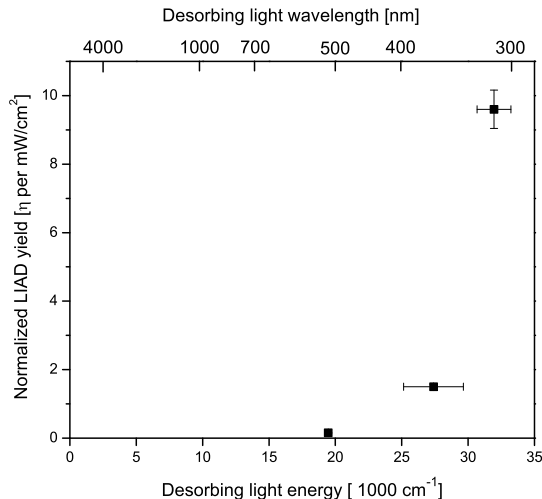


FIG. 11: Normalized maximum LIAD yield in Rb lockable stem cell (stem closed) as a function of desorbing light wavelength - 514 nm (Ar laser), 365 nm (filter FWHM=60 nm) and 313 nm (filter FWHM=25 nm).

the Cs atomic density change of  $\sim 1 \times 10^{10}$  atoms/cm<sup>3</sup> is realized. Unfortunately, there is no analogous control over the density ramp-down time, which is correspondingly lower,  $\approx 15$  s. Stabilization of the atomic density in the cell (stem closed) over a period of more than 20 minutes with an instability less than  $1.5 \times 10^9$  atoms/cm<sup>3</sup> is shown in Fig. 10. The lower trace on the plot shows the desorbing-light intensity. Note that the cell temperature variation during the entire cycle when the vapor density is increased with the help of LIAD by a factor of 1.5 is less than 0.5°C. Varying the cell temperature by  $\approx 3^\circ\text{C}$  would be required to achieve this vapor-density change thermally.

## IX. DISCUSSION AND CONCLUSION

We have explored the LIAD effect in paraffin-coated Rb, Cs, K, and Na cells extending the range of the desorption-light spectrum from visible to UV. We used lockable-stem cells in order to reduce, to a large degree, the relaxation of the alkali-atom density due to the stem. The main advantage of using the lockable-stem cells (stem closed) is the possibility of obtaining larger densities, for example, a factor of five gain in comparison with an open stem for Rb in our experiment. More importantly, one obtains a much longer density relaxation time ( $\tau_2$ ).

In the case of Rb and Cs, atoms with higher saturated vapor pressure at room temperature, irradiation with a few tens of mW/cm<sup>2</sup> of visible (514-nm) light causes significant LIAD effect. With Na and K cells and visible desorption light, no LIAD was observed.

Two different paraffins used with Rb do not show significant difference in the LIAD performance of the cells.

Experiments with UV light (365 nm and 313 nm) and a Rb lockable-stem cell show particularly high-yield LIAD. When using UV light at 365 nm, an order-of-magnitude gain in the yield of the desorption process ( $\eta$ ) is realized in comparison with using 514-nm light. Intensities as low as 0.25 mW/cm<sup>2</sup> at 313-nm light cause even stronger LIAD in Rb. Maximum LIAD yield in the Rb lockable-stem cell (stem closed) normalized to intensity [53] is plotted in Fig. 11 against the wavelength of the desorbing light - 514 nm (Ar laser), 365 nm (filter FWHM=60 nm) and 313 nm (filter FWHM=25 nm). A strong increase of the yield occurs towards shorter wavelengths.

In the case of K lockable-stem cell and UV desorbing light (365 nm) we registered much faster relaxation (short  $\tau_2$  time) of the vapor density compared to the case of Rb and Cs. Note that insufficient ripening is not a likely reason for the difference because K vapor pressure in the cell (open and closed stem configurations) was within 30 percents of saturated K vapor pressure at the same temperature.

We plan to extend the study of LIAD of alkali atoms in paraffin-coated cells towards the 200-nm range (with cells made of UV-transmitting glass). This will reveal whether the yield continues to increase for shorter wavelengths, or whether the presently observed dependence is the long-wavelength portion of a broad resonance. Indeed, resonant photodesorption was observed for some other systems, for example, CO on Ni [54] (resonance centered at 270 nm, FWHM=85 nm).

Combining the increased LIAD efficiency in the UV range with the use of closed-stem cells opens the door to practical applications, for example, for stabilizing or modulating the atomic density. Thus we may replace complicated (for example, non-magnetic) and high-power-consuming heating systems with a simple LIAD scheme with desorbing light produced with UV light-emitting diodes. This is demonstrated in this work with a Cs lockable-stem cell, see Figs. 10 and 9 that show stabilization and pulsing alkali-vapor density using LIAD. Such fast, high-contrast control of the vapor density is hard to achieve by heating/cooling the vapor cell.

LIAD may become a useful technique in the ongoing work aimed at developing highly miniaturized atomic frequency references [49, 50], magnetometers [51], and gyroscopes. These devices take advantage of miniature atomic vapor cells with physical dimensions on the order of 1 mm or smaller [20, 52]. In order to increase the signal in such miniaturized cells, an efficient method to elevate the atomic density is required. As it is shown in Ref. [30], compared to changing vapor densities by heating coated cells, LIAD may offer significant improvement in terms of spin-relaxation times.

### Acknowledgments

The authors would like to thank Joseph W. Tringe for providing the Blak-Ray discharge lamp and Luxco Wax for providing wax samples. This research was supported by the Office of Naval Research (grants N00014-97-1-0214 and SBIR), the Russian Foundation for Basic Research

(grant 03-02-17509 RFBR), the National Science Foundation, a Cal-Space Mini-grant, NURI grant HM1582-08-1-0006, Lawrence Berkeley National Laboratory's Nuclear Science Division, and the University of California at Berkeley's Undergraduate Research Apprenticeship Program.

- 
- [1] H. G. Robinson, E. S. Ensberg, and H. G. Dehmelt, *Bull. Am. Phys. Soc.* **3**, 9 (1958).
- [2] M. A. Bouchiat and J. Brossel, *Phys. Rev.* **147**, 41 (1966); M. A. Bouchiat, Ph. D. Thesis, University of Paris, 1964.
- [3] E. B. Alexandrov and V. A. Bonch-Bruevich, *Opt. Engin.* **31**, 711 (1992).
- [4] E. B. Alexandrov, M. V. Balabas, A. S. Pasgalev, A. K. Vershovskii, and N. N. Yakobson, *Laser Phys.* **6**, 244 (1996).
- [5] J. Dupont-Roc, S. Haroche and C. Cohen-Tannoudji, *Phys. Lett.* **28A**, 638 (1969); C. Cohen-Tannoudji, J. Dupont-Roc, S. Haroche, and F. Laloe, *Phys. Rev. Lett.* **22**, 758 (1969).
- [6] D. Budker, V. Yashchuk, and M. Zolotarev, *Phys. Rev. Lett.* **81**, 5788 (1998); D. Budker, D. F. Kimball, S. M. Rochester, and V. V. Yashchuk, *Phys. Rev. Lett.* **85**, 2088 (2000); D. Budker, D. F. Kimball, S. M. Rochester, V. V. Yashchuk, and M. Zolotarev, *Phys. Rev. A* **62**, 043403 (2000); D. Budker, D. F. Kimball, V. V. Yashchuk, and M. Zolotarev, *Phys. Rev. A* **65**, 055403 (2002).
- [7] E. B. Alexandrov, M. V. Balabas, A. K. Vershovskii, and A. S. Pasgalev, *Technical Physics* **49**(6), 779-783 (2004).
- [8] D. Budker, W. Gawlik, D. F. Kimball, S. M. Rochester, V. V. Yashchuk, and A. Weiss, *Rev. Mod. Phys.* **74**, 1153 (2002).
- [9] E. S. Ensberg, *Phys. Rev.* **153**, 36 (1967).
- [10] V. Yashchuk, D. Budker and M. Zolotarev, in *Trapped Charged Particles and Fundamental Physics* AIP Conference Proceedings 457, edited by D.H.E. Dubin and D. Schneider (American Institute of Physics, New York, 1999), pp. 177-181.
- [11] D. F. Kimball, D. Budker, D. S. English, C.-H. Li, A.-T. Nguyen, S. M. Rochester, A. Sushkov, V. V. Yashchuk, and M. Zolotarev, in *Art and Symmetry in Experimental Physics* AIP Conference Proceedings 596, edited by D. Budker, P. H. Bucksbaum, and S. J. Freedman (American Institute of Physics, New York, 2001), pp. 84-107.
- [12] D. Budker, D. F. Kimball, S. M. Rochester, and V. V. Yashchuk, *Phys. Rev. Lett.* **83**, 1767 (1999).
- [13] L. J. Wang, A. Kuzmich, and A. Dogariu, *Nature* **406**, 277 (2000).
- [14] A. Kuzmich, L. Mandel, and N. P. Bigelow, *Phys. Rev. Lett.* **85**, 1594 (2000).
- [15] B. Julsgaard, J. Sherson, J. Ignacio Cirac, Jaromir Fiurasek, and E. S. Polzik, *Nature* **432**, 482 (2004).
- [16] J. F. Sherson, H. Krauter, R. K. Olsson, B. Julsgaard, K. Hammerer, I. Cirac, and E. S. Polzik, *Nature* **443**, 557 (2006).
- [17] V. V. Yashchuk, D. Budker, W. Gawlik, D. F. Kimball, Yu. P. Malakyan, and S. M. Rochester, *Phys. Rev. Lett.* **90**, 253001 (2003).
- [18] V. M. Acosta, M. Auzinsh, W. Gawlik, P. Grisins, J. M. Higbie, D. F. Jackson Kimball, L. Krzemien, M. P. Ledbetter, S. Pustelny, S. M. Rochester, V. V. Yashchuk, and D. Budker, <http://arxiv.org/abs/0709.4283>.
- [19] D. Budker, L. Hollberg, D. F. Kimball, J. Kitching, S. Pustelny, and V. V. Yashchuk, *Phys. Rev. A* **71**, 012903 (2005).
- [20] M. V. Balabas, D. Budker, J. Kitching, P. D.D. Schwindt, and J. E. Stalnaker, *JOSA B* **23**(6), 1001 (2006).
- [21] M. A. Bouchiat, Ph. D. thesis, L'Universite de Paris (1964).
- [22] H. Gibbs, *Phys. Rev.* **139**, 1374 (1965).
- [23] V. Liberman and R. J. Knize, *Phys. Rev. A* **34**, 5115 (1986).
- [24] M. V. Balabas, M. I. Karuzin, and A. S. Pasgalev, *JETP Lett.* **70**, 196 (1999).
- [25] J. Vanier, J.-F. Simard, and J.-S. Boulanger, *Phys. Rev. A* **9**(3), 1031 (1974).
- [26] E. B. Aleksandrov, M. V. Balabas, A. K. Vershovskii, A. I. Okunevich, and N. N. Yakobson, *Optics and Spectroscopy*, **87**(3), 329-34 (1999).
- [27] A. Gozzini, F. Mango, J. H. Xu, G. Alzetta, F. Maccarrone, and R. A. Bernheim, *Nuovo Cimento D* **15**, 709 (1993).
- [28] E. Mariotti, S. Atutov, M. Meucci, P. Bicchi, C. Marinelli, and L. Moi, *Chem. Phys.* **187**, 111 (1994).
- [29] E. B. Alexandrov, M. V. Balabas, D. Budker, D. English, D. F. Kimball, C.-H. Li, and V. V. Yashchuk, *Phys. Rev. A* **66**, 042903 (2002).
- [30] M. T. Graf, D. F. Kimball, S. M. Rochester, K. Kerner, C. Wong, D. Budker, E. B. Alexandrov, M. V. Balabas, and V. V. Yashchuk, *Phys. Rev. A* **72**, 023401 (2005).
- [31] I. N. Abramova, E. B. Aleksandrov, A. M. Bonch-Bruevich, and V. V. Khromov, *Pis'ma Zh. Eksp. Teor. Fiz.* **39**, 172 (1984) [*JETP Lett.* **39**, 203 (1984)].
- [32] A. M. Bonch-Bruevich, Yu. N. Maksimov, S. G. Przhibel'skiĭ, and V. V. Khromov, *Zh. Eksp. Teor. Fiz.* **92**, 285 (1987) [*Sov. Phys. JETP* **65**, 161 (1987)].
- [33] A. M. Bonch-Bruevich, T. A. Vartanyan, Yu. N. Maksimov, S. G. Przhibel'skiĭ, and V. V. Khromov, *Zh. Eksp. Teor. Fiz.* **97**, 1761 (1990) [*Sov. Phys. JETP* **70**, 993 (1990)].
- [34] M. Meucci, E. Mariotti, P. Bicchi, C. Marinelli, and L. Moi, *Europhys. Lett.* **25**, 639 (1994).
- [35] J. H. Xu, A. Gozzini, F. Mango, G. Alzetta, and R. A. Bernheim, *Phys. Rev. A* **54**, 3146 (1996).
- [36] S. N. Atutov, V. Biancalana, P. Bicchi, C. Marinelli, E. Mariotti, M. Meucci, A. Nagel, K. A. Nasyrov, S. Rachini, and L. Moi, *Phys. Rev. A* **60**, 4693 (1999).

- [37] S. Gozzini and A. Lucchesini, *Eur. Phys. J. D* **28** 157-162, (2004).
- [38] A. Hatakeyama, K. Oe, K. Ota, S. Hara, J. Arai, T. Yabuzaki, and A. R. Young, *Phys. Rev. Lett.* **84**, 1407 (2000).
- [39] A. Hatakeyama, K. Enomoto, N. Sugimoto, and T. Yabuzaki, *Phys. Rev. A* **65**, 022904 (2002).
- [40] J. Brewer and H. G. Rubahn, *Chem. Phys.* **303**(1-3), 1-6 (2004).
- [41] A. Burchianti, C. Marinelli, A. Bogi, J. Brewer, K. Rubahn, H. G. Rubahn, F. Della Valle, E. Mariotti, V. Biancalana, S. Veronesi, and L. Moi, *Europhysics Letters* **67**(6), 983-989 (2004).
- [42] A. Cappello, C. de Mauro, A. Bogi, A. Burchianti, S. Di Renzone, A. Khanbekyan, C. Marinelli, E. Mariotti, L. Tomassetti, and L. Moi, *The Journal of Chem. Physics* **127**, 044706 (2007).
- [43] S. J. Seltzer and M. V. Romalis, Private Communication.
- [44] S. Ghosh, A. R. Bhagwat, C. K. Renshaw, S. Goh, A. L. Gaeta, and B. J. Kirby, *Phys. Rev. Lett.* **97**, 023603 (2006).
- [45] M. V. Balabas and S. G. Przhibelskii, *Chem. Phys. Reports* **14** (6), 882-889 (1995).
- [46] S. Gozzini, A. Lucchesini, L. Marmugi, and G. Postorino, *Eur. Phys. J. D* **47**, 1-5 (2008).
- [47] E. Mariotti, S. Atutov, M. Meucci, P. Bicchi, C. Marinelli and L. Moi, *Chemical Physics* **187**, 111 (1994).
- [48] C. Klempt, T. van Zoest, T. Henninger, O. Topic, E. Rasel, W. Ertmer, and J. Arlt, *Phys. Rev. A* **73**, 013410 (2006).
- [49] J. Kitching, S. Knappe, and L. Hollberg, *Appl. Phys. Lett.* **81**, 553 (2002).
- [50] Y. Y. Jau, A. B. Post, N. N. Kuzma, A. M. Braun, M. V. Romalis, and W. Happer, *Phys. Rev. Lett.* **92**, 110801 (2004).
- [51] P. Schwindt, S. Knappe, V. Shah, L. Hollberg, J. Kitching, L. Liew, and J. Moreland, *Appl. Phys. Lett.* **85**, 6409 (2004).
- [52] L. Liew, S. Knappe, J. Moreland, H. G. Robinson, L. Hollberg, and J. Kitching, *Appl. Phys. Lett.* **84**, 2694 (2004).
- [53] The normalization for the three wavelengths used suppose linear dependence of the yield on the desorption light intensity. We verified the linearity for the case of 365-nm desorbing light (in the interval of 1 to 10 mW/cm<sup>2</sup>). In Ref. [29] a nonlinear behavior of the yield is registered at low desorption intensity in open-stem cells. We did not observe such behavior in rubidium lockable-stem cell (stem closed) at 365-nm desorbing light.
- [54] R. O. Adams and E. E. Donaldson, *The Journal of Chem. Physics* **42** (2), 770-774 (1965).